

Electronic and nuclear effects in ion-induced desorption from NaCl{100}

Z. Postawa,^{a)} R. Maboudian, M. El-Maazawi, M. H. Ervin, M. C. Wood, and N. Winograd

Department of Chemistry, The Pennsylvania State University, University Park, Pennsylvania 16802

(Received 5 August 1991; accepted 8 November 1991)

Multiphoton resonance ionization (MPRI) spectroscopy has been employed to investigate the ejection mechanisms of neutral and ionic particles from an ion-bombarded NaCl{100} single crystal. The results are used to reveal the similarities and the differences between ion bombardment and electron irradiation of alkali halides. The mass spectra of neutral species and positive and negative ions have been measured. The yield of Na⁺ ions is found to be two orders of magnitude higher than in measurements with electron bombardment. It is suggested that the secondary ions are created by direct emission from the collision cascade. The ejection of neutral Na atoms is observed to be very sensitive to the temperature of the target, the angle of incidence, and the state of the surface as determined by the time-of-flight (TOF) measurements. In particular, it is found that most of the neutral Na atoms are emitted with thermal energies, which indicates that desorption via electronic transitions dominates over ejections from collision cascades. The relative yield of the collisional component to the thermal component is found to vary significantly as the surface structure is modified. This investigation emphasizes the importance of measurements with low incident-ion dose which allows one to decouple the single ion/surface interaction from the accumulative effect of ion-induced surface modifications.

I. INTRODUCTION

The interaction of energetic electrons with solid surfaces has been investigated for several decades.¹ Due to their simple crystallographic and electronic structures, alkali halides have been widely used as model systems for studying the electronic interactions. It is generally accepted that the first step in the conversion of the energy deposited into the electronic system of the crystal is the creation of a self-trapped exciton (STE).²⁻⁵ In alkali halides, the self-trapped exciton is regarded as an electron bound to a covalently bonded diatomic halogen molecular ion.

The nonradiative decay of the STE into a halogen vacancy (*F* center) and an interstitial halogen atom (*H* center) leads to desorption. Williams *et al.* have distinguished between two types of *F-H* pair formation—a diffusive thermally activated process and a dynamic one.⁵ The thermal mechanism proceeds via diffusion of a halogen atom out of the relaxed STE in its lowest π -luminescence state. This process ends by the thermal evaporation of the diffusing neutral halogen atom. In the dynamic process, the energy of the *F-H* pair formation is derived from the energy stored in the higher excitonic state of the STE. If such an event occurs in close proximity to the surface, it can lead to the emission of a nonthermal halogen atom. If, instead, the dynamic process occurs deeper in the bulk, it produces an *H* center which can reach the surface by thermal diffusion and contribute to the thermal emission.⁶ The desorption of the halogen atoms by these two processes leads to the formation of a surface layer enriched in alkali ions. These ions can subsequently be neutralized by secondary electrons or by recombining with the *F*

centers.⁷ Since neutral alkali atoms are bound loosely to the surface, they simply evaporate.

Apart from the ejection of neutral atoms, a variety of molecular and ionic species have also been observed during the electron bombardment of alkali halides.⁸⁻¹⁰ In these measurements, the ratio of the alkali ion yield to alkali atom yield was determined to be in the 10⁻⁵–10⁻⁷ range.^{8,11} These results have been explained in terms of the Knotek–Feibelman-like mechanism^{9,10,12} as well as the gas-phase ionization of the neutral species.⁸

This class of materials is one of the few systems in which the nuclear (collision cascade) and the electronic processes coexist efficiently for the same incident ion energy.³ Hence, ion bombardment of alkali halides provides a fascinating system for examining the competition between the nuclear and electronic channels of desorption. Recent results indicate that during low-energy ion bombardment of alkali halide crystals, neutral atoms are ejected predominantly due to electronic processes.¹³⁻¹⁵ Using the Doppler shift laser-induced fluorescence technique (DSLIF), Yu *et al.* found that the energy distribution of sodium atoms sputtered from NaCl single crystal by 15 keV Ar⁺ bombardment was entirely thermal.¹⁴ More recently, similar spectra have been reported by other groups.^{14,15} In all these measurements, the results are in clear conflict with the earlier data obtained on compressed-powder samples.¹⁶⁻¹⁹ The time-of-flight measurements^{16,17} as well as the DSLIF work^{18,17} on polycrystalline samples showed significant contribution from the collision cascade in addition to the thermal component.

Several plausible explanations have been proposed to resolve the conflict between the compressed-powder samples and the single-crystal results. First, in a single crystal, a large fraction of the incident ions can be channeled deep into the bulk.²⁰ In this way, the nuclear stopping power close to

^{a)} Permanent address: Institute of Physics, Jagellonian University, ulica Reymonta 4, PL-30-059 Kraków 16, Poland.

the surface is reduced. However, the electronic processes are less affected by channeling, since in this case, the interactions occur due to long-range electromagnetic forces. As a result, in a single crystal, the electronic processes could contribute more to the sputtering than the collisional mechanism. Second, the oxygen confined in a compressed-powder sample during pellet creation could combine with the neutral alkali atoms at the surface and hence reduce the evaporation of the alkalis.²¹ This process can lead to the suppression of the thermal component in polycrystalline targets because oxygen can combine with neutral sodium and prevent it from evaporation. Experimental verification of these ideas requires detailed measurements on well-characterized surfaces.

In addition, the ionic emission during ion bombardment of alkali halides has not been studied till recently.²² This process might have a different nature than for electron bombardment and may resemble the ionic ejection from metal surfaces. However, since the alkali halides are ionic crystals with a nearly empty conduction band, one might expect a substantially higher ionic yield when compared to metals.

In this paper, multiphoton resonance ionization (MRPI) spectroscopy is employed to systematically probe the neutral and ionic particles ejected from an ion bombarded surface of an NaCl{100} single crystal. The extreme efficiency of the resonant ionization technique coupled with a position-sensitive detector enables us to measure the angle-resolved time-of-flight distributions of ejected neutrals with low doses of bombarding ions ($< 10^{13}$ ions/cm²). Under these conditions, the crystallographic structure of the investigated surface is preserved. Low ion fluence also minimizes any modification of the surface composition due to preferential sputtering.²⁰

We have investigated the influence of the target temperature and crystalline structure on the ejection of neutral sodium atoms. We have observed contributions from both nuclear and electronic processes to the mission process. Our results strongly suggest that the relative yield of these two desorption channels is influenced by the state of the surface. These measurements emphasize the importance of low dose measurements.

The mass spectrum of neutral species and positive and negative ions has been determined. The comparison between the ionic and the neutral mass spectra indicates that the mechanisms proposed for the ejection of secondary ions from electron-irradiated alkali halides are not operating in the ion-bombardment process. It is suggested that direct ejection of ions from the collision cascade plays a significant role in this case. The emission of sodium dimers from NaCl{100} has also been investigated. The data indicate that Na₂ is created above the surface, in contrast to the intact dimer emission mechanism proposed for halogen molecules.^{17,23}

II. EXPERIMENT

The experiment was performed under ultrahigh vacuum conditions using either an energy- and angle-resolved neutral (EARN) detector, or a reflecting mirror analyzer (RMA). The EARN chamber (base pressure 2×10^{-10}

Torr) is equipped with low-energy electron diffraction (LEED) and Auger electron spectroscopy (AES). This system has been employed to measure the angle-resolved time-of-flight distributions of ejected neutral particles. The RMA apparatus (base pressure 4×10^{-9} Torr) was used to determine the neutral as well as the positive and negative secondary ion mass spectra (SIMS).

An optical quality NaCl{100} crystal was cleaved in air and subsequently cleaned by heating to 660 K in an ultrahigh vacuum for several hours. This procedure is known to produce a well-ordered, single crystal surface as examined by LEED and AES.²⁴ The sample temperature was monitored by an chromal-alumel thermocouple attached to the crystal.

The details of the two experimental setups have been described elsewhere.^{25,26} In short, the EARN measurements proceed as follows: A pulse of 5 keV Ar⁺ ion beam is focused onto a 2 mm diameter spot on the sample. A given time after the ion impact, a ribbon-shaped laser pulse resonantly ionizes a small volume of the desorbed neutrals, thus defining the time of flight of the probed species. The ionization schemes used in this investigation are presented in Fig. 1.^{27,28} The ionized particles are then accelerated toward a position-sensitive microchannel plate detector and are displayed on a phosphor screen. The image is, in turn, monitored by a

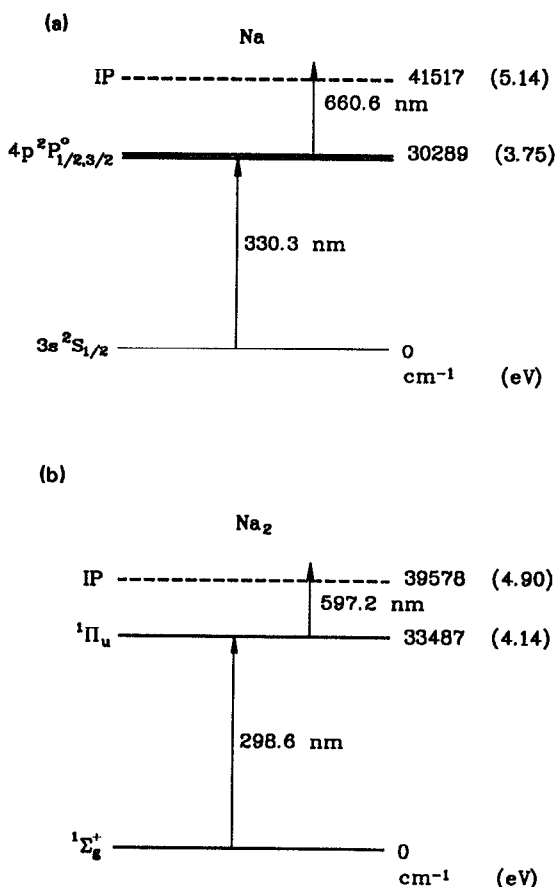


FIG. 1. The ionization schemes used to resonantly ionize (a) sodium atoms and (b) sodium dimers.

charge-couple-device camera which is interfaced to a micro-VAX II computer for data storage and processing. For a typical spectrum, 50 images, each corresponding to a different velocity time of flight, are collected and sorted into an intensity map of kinetic energies and take-off angles using a deconvolution procedure described earlier.²⁵

With the RMA setup, atoms and molecules are sputtered by a pulse of 6.5 keV Ar ion beam at 45° incidence. The ejected neutral species may be ionized either resonantly (MPRI) using UV photons from a Nd:YAG pumped dye laser, or nonresonantly by focusing the fourth harmonic of the Nd:YAG laser (wavelength of 266 nm). The photoions are accelerated into a time-of-flight RMA and are detected using a chevron microchannel plate. Furthermore, by simply blocking the laser beam and adjusting the reflecting potentials of the electrostatic mirror, positive secondary ions can be detected. Although the absolute yields cannot be determined, the ratio of the positive ion yield to the neutral yield can be deduced by comparing the peak areas in the SIMS distribution to the respective peaks in the MPRI spectrum. For this purpose, both distributions are first normalized to the incident ion current. In addition, the peak intensities in the MPRI spectrum are corrected for the spatial overlap of the laser beam with the ion-desorbed plume and also for the laser power density required for 100% ionization of the neutral species.²⁶ By modifying the extraction field, negative secondary ions can also be detected. However, in this case, the transmission of the mass spectrometer is different and unknown; hence, neither the absolute negative nor relative ion fraction can be determined.

III. RESULTS AND DISCUSSION

The mass spectrum of neutral particles ejected from 6.5 keV Ar⁺ bombarded NaCl{100} at room temperature is presented in Fig. 2(a). The spectrum is obtained using the nonresonant ionization technique. Since the ionization cross sections for different species are not known, it is difficult to compare the relative yields of various particles. Furthermore, the cluster signals are influenced by laser-induced fragmentation. The dominating features in the mass distribution are peaks due to Na and Cu. The Cu peak originates from the sample holder. The Cl atomic peak is missing, presumably due to its high ionization potential of 13 eV. In addition to atomic emission, a significant contribution from Na₂ is observed. Similar species have been observed during the electron bombardment of NaCl.⁸

The mass spectrum of the positive ions ejected by bombardment of NaCl{100} with 6.5 keV Ar⁺ is shown in Fig. 2(b). Only three peaks are present corresponding to Na⁺, Na₂Cl⁺, and Na₂⁺. Unlike the results obtained from electron bombardment,⁸ no Cl⁺ is observed. In general, two mechanisms have been proposed to describe the creation of positive ions from electron-bombarded alkali halides. At low temperatures, it is believed that internal Auger-like transitions could lead to the emission of positive ions.^{12,29} At higher temperatures where evaporation becomes important, gas-phase ionization of ground-state neutrals by primary and secondary electrons becomes the dominant ionization process.⁸ The absence of a Cl⁺ peak in our mass spectrum sug-

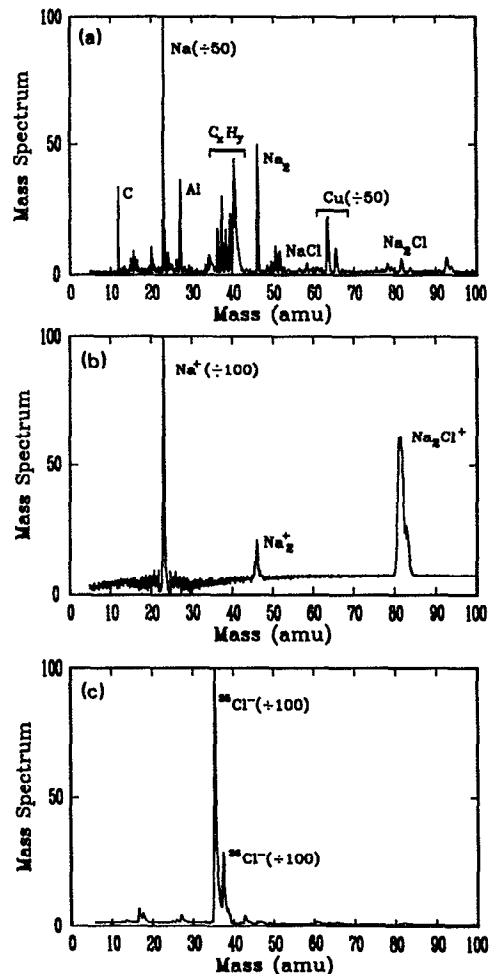


FIG. 2. The mass spectrum of (a) neutral particles; (b) positive; and (c) negative ions emitted from 6.5 keV Ar⁺ ion-bombarded NaCl{100} at room temperature. The spectra are normalized to the intensity of the most prominent peaks.

gests that in the case of ion bombardment of NaCl, neither of these two mechanisms is operating. Furthermore, it was found that the positive ion fraction was as low as 10⁻⁶ for electron bombardment.^{8,9} Using the RMA apparatus, the ratio of the Na⁺ ion yield to the Na atom yield was determined to be about $(3 \pm 2) \times 10^{-4}$. This fraction is measurably higher than that observed during electron irradiation of alkali halides,⁸ or in ion bombardment of metals.³⁰ Furthermore, such a large ionic contribution rules out the possibility of gas-phase ionization by secondary electrons.³¹ However, unlike bombardment by electrons where only low energy particles are desorbed, during ion bombardment, energetic atoms are ejected from the collision cascade.²⁰ The NaCl lattice is composed of positive and negative ions and hence one would expect for the particles in the collision cascade to be primarily ionic. Since the conduction band in this material is nearly empty, the neutralization process is less efficient than for metals. This might explain the abnormally high relative secondary ion yields observed in our experiment. This hypothesis is supported additionally by the negative ion mass spectrum [Fig. 2(c)] in which Cl⁻ is the only domi-

nant feature. The main implication of the above hypothesis is that the secondary ions should be emitted with energies characteristics of the collision cascade which is, indeed, observed experimentally.²²

It has been reported that Na atoms ejected from ion-bombarded NaCl single crystal have only a thermal distribution.¹³⁻¹⁵ These results are in contradiction to the earlier measurements on polycrystalline samples where significant collisional contribution was observed.¹⁶⁻¹⁹ To help resolve this discrepancy, the time-of-flight distributions of Na atoms emitted from an ion-bombarded NaCl{100} surface at several target temperatures have been measured (Fig. 3). For these investigations, a 5 keV Ar⁺ ion beam at normal incidence is employed and only particles ejected along the <111> crystallographic direction are collected. Two components are visible in the spectra. The distributions at small times of flight can be described by a Thompson formula with a surface binding energy of about 1.5 eV which indicates that particles contributing to this part of the spectrum originate from the collision cascade.¹⁹ Moreover, this component appears not to depend on the target temperature. In contrast, the feature at times greater than 5 μ s is very sensitive to the

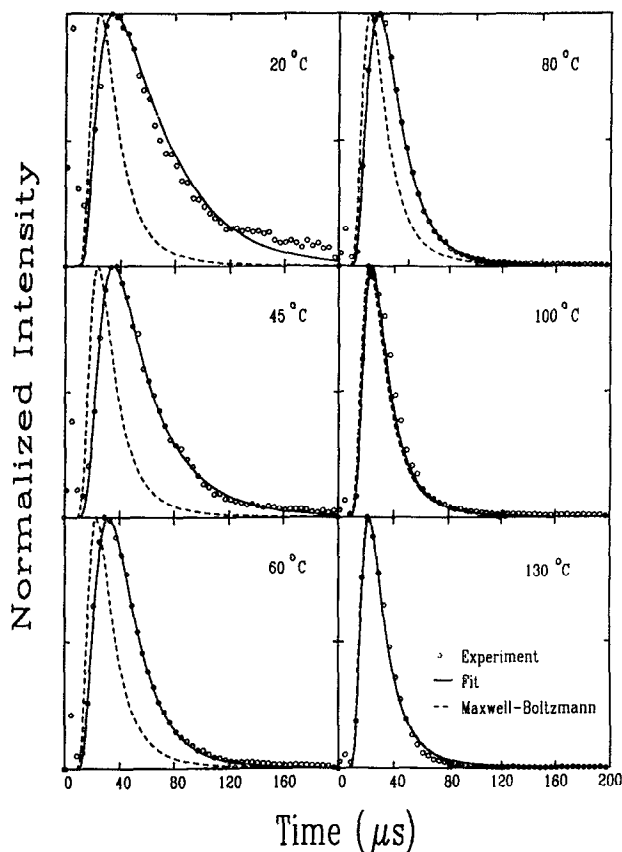


FIG. 3. The time-of-flight distributions of sodium atoms emitted from ion-bombarded NaCl{100} at various target temperatures. The 5 keV Ar ion beam is perpendicular to the surface and only particles ejected along the <111> crystalline direction are collected. All spectra are normalized to the intensity of the thermal peak. The solid line represents the best fit of Eq. (3) to the thermal part of the spectrum. The dashed line is the Maxwell-Boltzmann distribution with the parameter T equal to the measured surface temperatures.

temperature of the sample. For temperatures higher than 100 °C, this part of the spectrum can be described by the Maxwell-Boltzmann distribution $d\Phi(E)/dE$

$$d\Phi(E)/dE \propto E \exp(-E/k_B T), \quad (1)$$

or in time representation²⁵

$$d\Phi(t)/dt \propto t^{-4} \exp(-mL^2/2k_B T t^2), \quad (2)$$

where E is the atom's kinetic energy, k_B is the Boltzmann constant, T is the sample temperature, m is the mass of the emitted particle, L is the flight path (~ 1.5 cm), and t is the measured time of flight. At high temperatures, fitting this formula to the experimental data results in a temperature which agrees well with the measured value. However, as the target temperature is lowered, the measured spectra begin to deviate from a simple Maxwell-Boltzmann distribution.

A similar behavior has been observed previously in the experiments with electron bombardment.^{32,33} In the experiments on LiF, Green *et al.* observed time delays up to several hundreds of microseconds.⁷ Delays as long as minutes were observed by Betz *et al.*³³ According to the proposed models, the rate of emission of neutral alkali atoms is determined by the diffusion coefficients of H or F centers, and by the residence time of the alkalis on the surface.^{3-5,23} Both of these parameters are strongly temperature dependent. The lower the surface temperature, the smaller the diffusion coefficient and also the longer the time the alkali atoms spend on the surface.

Using a velocity selector combined with a time-of-flight spectrometer, Overeijnder *et al.* have measured the time delays occurring in the desorption of alkali atoms from polycrystalline surfaces bombarded with a 540 eV electron beam.³² They observed in most cases that two delayed components appear in the TOF spectrum. To estimate numerically the observed delays, they assumed that the response from the surface could be expressed by two exponential terms of the form $\tau_i^{-1} \exp(-t/\tau_i)$, where τ_i is a relaxation time. In this case, the shape of the experimental time-of-flight distribution was described by

$$\frac{dF(t)}{dt} \propto \int_0^t dt' \frac{d\Phi(t-t')}{dt'} \sum_{i=1}^2 c_i \exp\left(-\frac{t'}{\tau_i}\right), \quad (3)$$

where $d\Phi(t)/dt$ is given by Eq. (2) and c_i are constants. Similar to Overeijnder *et al.*, we find that, at temperatures lower than 100 °C, two exponential factors are needed to obtain a satisfactory fit to the measured spectra. The results are shown in Table I. However, the time delays observed in

TABLE I. The parameters obtained from the best fit of Eq. (3) to the experimental distributions measured at various target temperatures. The NaCl{100} is bombarded by a 5 keV Ar⁺ ion beam at normal incidence.

T_{measured} (°C)	T_{fit} (°C)	C_1	C_2	τ_1 (μ s)	τ_2 (μ s)
20	22	1	14.0	34.0	0.7
45	46	1	2.2	28.0	7.8
60	62	1	11.7	12.0	0.2
80	79	1	6.2	4.0	0.6
100	101	1	8.0	1.0	0.05
130	133	1	0.0	0.7	...

our experiment are much shorter than those reported previously (e.g., more than 300 μs for NaCl).³² This discrepancy might be due to the fact that, at a given temperature, the time delay of atomic emission depends strongly on the penetration depth of the incident projectile. This depth is much shorter for a 5 keV Ar^+ ion than for a 540 eV electron and hence, in the former case, diffusion processes are faster.³⁴ Desorption with long time delays (τ larger than 100 s on LiF), as observed by Betz *et al.*,³³ cannot be probed in our experiment.

By integrating the areas under the curves in Fig. 3, the dependence of the thermal S_{th} and the collisional S_{col} components on the target temperature can be determined. As is shown in Fig. 4, the yield is already saturated at 80 $^{\circ}\text{C}$. This contradicts the previous experiments with Ar ions and electrons, in which the plateau was not reached even at 200 $^{\circ}\text{C}$.^{14,35} The beam-induced changes in surface stoichiometry are potentially responsible for this discrepancy. In the previous measurements, the surface was bombarded by a continuous beam with an average fluence of 10^{15} – 10^{17} ions/cm². In electron bombardment experiments, it is shown that a high incident dose leads to a surface layer enriched in sodium.³⁵ In this case, the emission of Na atoms is controlled more by the evaporation rate of the alkali atoms than by the rate of defect creation. In our measurements, the total dose is less than 10^{13} ions/cm² (2×10^6 ions/cm² in a 150 ns pulse). Under these conditions, the balance between the rate of evaporation and the rate of defect formation can be reached at much lower temperatures.

In Table II, the relative sputtering yield of the thermal to the nonthermal atoms are presented. This ratio varies from 0.092 at 20 $^{\circ}\text{C}$ to 0.023 at 130 $^{\circ}\text{C}$. This differs from the previous data on NaCl single crystals where no collisional component was observed, even at room temperature.^{13–15}

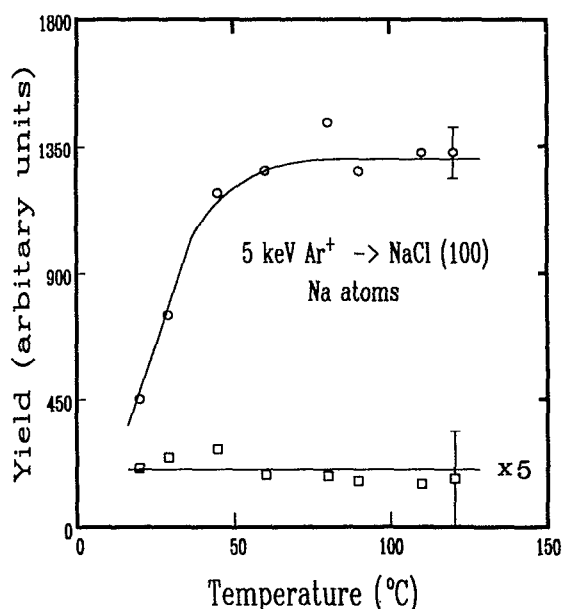


FIG. 4. The dependence of the thermal (O) and the collisional (□) contributions on the target temperature. The solid line is drawn only as an aid to the eye.

TABLE II. The ratio of the collisional S_{col} to the thermal S_{th} sputtering yields from a 5 keV Ar^+ ion-bombarded NaCl{100} surface at various target temperatures. The polycrystalline data are taken from Ref. 13. In that experiment, the NaCl sample was bombarded with a 20 keV Ar^+ ion beam.

Temperature ($^{\circ}\text{C}$)	Single crystal $S_{\text{col}}/S_{\text{th}}$ (%)	Polycrystal $S_{\text{col}}/S_{\text{th}}$ (%)
20	9.2	26.0
40	5.0	
60	3.0	
80	2.5	
100	2.3	
130	2.3	

However, in those experiments, as mentioned earlier, a continuous ion beam with a higher energy was used which could locally increase the target temperature. As shown in Fig. 3, even a small increase in temperature leads to a significant enhancement in the thermal component relative to the collisional component. Furthermore, the DSLF technique was used in the above measurements. It has been suggested that the interference due to hyperfine splitting may reduce the resolution in the velocity measurements.¹⁵ This, along with the problem of high ion beam dose, could obscure the relatively small contribution from the collision cascade.

The collisional contribution obtained in our measurements is still considerably smaller than reported on compressed-powder targets (see Table II). One phenomenon that would explain this discrepancy is the channeling of the incident beam. This hypothesis can be verified by investigating the dependence of the TOF distribution on the azimuthal direction of the incident beam. As shown in Fig. 5, we have examined a geometry where the polar angle of incidence is fixed at 45° with respect to the surface normal and the azimuthal angle of incidence φ_i is varied. The target is held at room temperature and only Na atoms ejected perpendicular to the surface are recorded. The resulting spectra for $\varphi_i = 0^{\circ}$ ($\langle 101 \rangle$), $\varphi_i = 45^{\circ}$ ($\langle 111 \rangle$), and $\varphi_i = 22^{\circ}$ are then recorded. In a cubic lattice, these directions correspond to different degrees of "openness," ranging from very open for $\varphi_i = 0^{\circ}$ to nearly random for $\varphi_i = 22^{\circ}$. Compared to the spectra taken at normal ion incidence (Fig. 3), the present geometry enhances the collisional component relative to the thermal contribution. Furthermore, the ratio of the collisional yield S_{col} to the thermal yield S_{th} depends on the azimuthal angle of incidence and is maximum at $\varphi_i = 22^{\circ}$. This behavior can be understood in view of the fact that the projectiles incident along the open channels penetrate deeper into the crystal. As a consequence, the nuclear stopping power is reduced in the vicinity of the surface.²⁰ In contrast, electronic processes occur due to long-range electromagnetic forces for which channeling has less influence. The $\langle 111 \rangle$ crystallographic direction is more close packed than the $\langle 101 \rangle$ direction. This leads to a large collisional contribution along $\varphi_i = 45^{\circ}$ as compared to $\varphi_i = 0^{\circ}$, in good agreement with our results. The particles incident along the $\varphi_i = 22^{\circ}$ are channeled the least. Consequently, in this case, the collisional component is the most prominent. These results indicate that the channel-

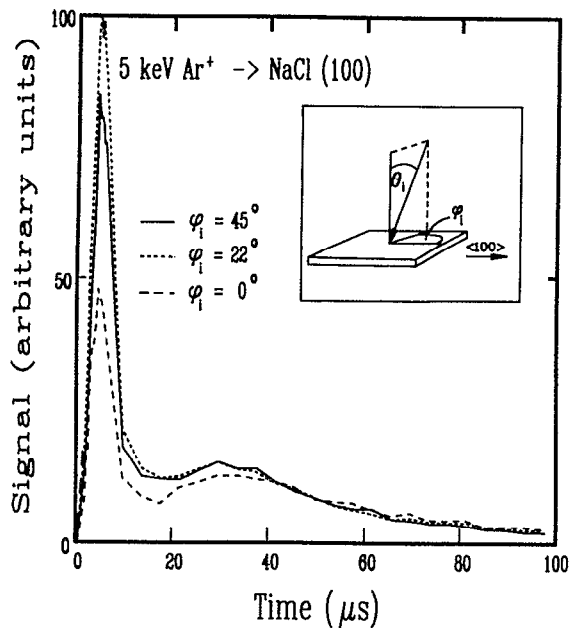


FIG. 5. The time-of-flight distributions of Na atoms emitted from the ion-bombarded NaCl{100} surface. The target is held at 20 °C. The spectra correspond to three different azimuthal directions φ , of the incident 5 keV Ar^+ beam. The polar angle of incidence θ , is fixed to be 45° with respect to the surface normal. Only particles emitted perpendicular to the surface are recorded. Spectra are not normalized.

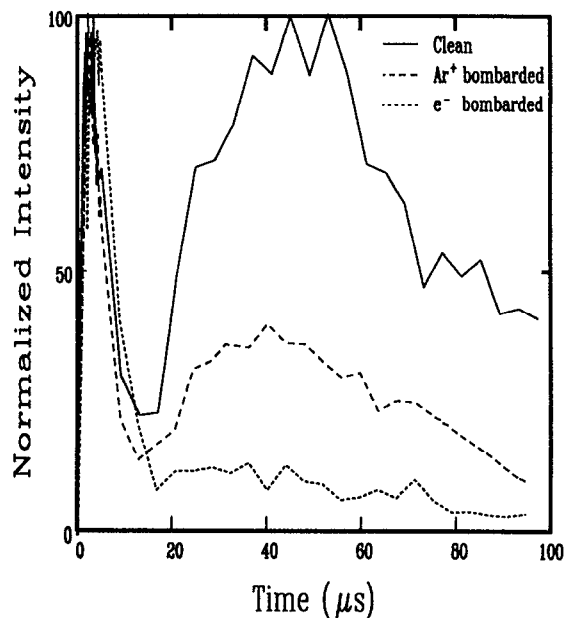


FIG. 6. The time-of-flight distributions of sodium atoms emitted from NaCl{100} at room temperature. The solid line represents the spectrum collected from the unaltered surface. The spectra obtained from the surface modified by bombardment with continuous ion ($5 \mu\text{A}/\text{cm}^2$ for 20 min) and electron ($100 \mu\text{A}/\text{cm}^2$) beams are represented by dashed and dotted lines, respectively. The distributions are normalized to the intensity of the collisional peak.

ing of the incident ion does play a significant role in the ratio of thermal to nonthermal yields. However, the effect of the incident azimuth is not large enough to fully resolve the discrepancy between the single crystal and the polycrystalline data. It must be kept in mind that even bombardment along the $\varphi_i = 22^\circ$ is not completely equivalent to the experiments done on polycrystalline samples.

To probe how the state of the surface influences the TOF distributions, the surface was exposed to 100 L of O_2 . It has been reported that exposure to O_2 reduces the thermal component in the velocity spectrum obtained from polycrystalline samples.²¹ In our case, this procedure did not lead to significant changes in the relative yield of the collisional to the thermal components. Only, the total signal was slightly reduced. However, it is not certain if O_2 was adsorbed on the surface by this procedure,³⁶ particularly in view of the fact that no additional diffraction spots were observed in the LEED pattern.

The surface was then modified by bombardment with a continuous ion beam ($5 \mu\text{A}/\text{cm}^2$ for 20 min) and then with a continuous electron beam ($100 \mu\text{A}/\text{cm}^2$ for 20 min). As shown in Fig. 6, both ion and electron beams altered the TOF distributions. The collisional component is enhanced by a factor of 2.5 after ion bombardment and by a factor of 8 after electron irradiation. In the latter case, only the collisional component remains in the TOF spectrum. This behavior can be due to the randomization of the surface region as well as to a change in surface composition. As was emphasized earlier, the randomization of the surface region eliminates the influence of ion channeling. Moreover, the creation

of a layer enriched in alkali atoms enhances the probability for ejection of loosely bound neutral Na atoms due to collisional processes. However, the ion-induced modifications of surface stoichiometry is considerably less effective than in the case of electron bombardment due to the removal of excess Na atoms by collisional sputtering. Hence, the ratio of nonthermal to thermal emission is higher after electron irradiation than after ion bombardment. Furthermore, our results indicate that the discrepancy between the single crystal and the polycrystalline sample is not as severe as reported earlier and the difference can be understood in terms of the influence of ion channeling combined with the state of the surface.

The ejection mechanisms of clusters in an ion bombardment process has been of longstanding interest.^{37,38} The neutral mass spectrum shown in Fig. 2 indicates a significant emission of Na_2 dimers. To determine its mechanism or emission, multiphoton resonant ionization spectroscopy was employed to measure the TOF distribution of Na_2 . Although the laser wavelength was tuned to a known Na_2 transition (see Fig. 1 and Ref. 28) and the frequency scan of the ionizing radiation showed a very broad, multicomponent absorption band, no signal at the mass of Na dimer was observed. Instead, a very strong signal was present at the mass of atomic sodium indicating that all the Na_2 dimers were photofragmented during the ionization process.

The TOF distribution of Na produced by photofragmentation of Na_2 is shown in Fig. 7. In the same figure, the TOF spectrum of neutral Na atoms is presented. For these measurements, the target is held at 130 °C. Surprisingly, the

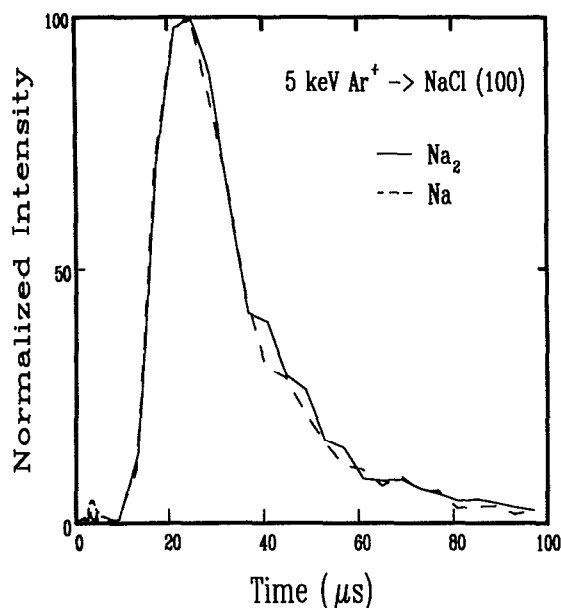


FIG. 7. The time-of-flight distributions of Na_2 dimers (solid line) and Na atoms (dashed line) emitted from ion-bombarded $\text{NaCl}\{100\}$ at 130°C .

two distributions look strikingly similar. It has been suggested that halogen molecules ejected by electron or ion bombardment are created by the recombination of halogen atoms at the crystal surface.^{17,23} However, this model cannot explain our data. If Na_2 dimers are created at the surface, they must have the same energy spectrum as Na atoms. Since the mass of Na_2 is twice the mass of atomic Na, the TOF distribution of Na_2 must, in this case, be shifted towards longer times. Since the monomer and the dimer TOF spectra are similar, Na_2 must be formed above the original surface plane, but still within the interaction range of the solid in order for the excess kinetic energy to be removed.³⁸

IV. CONCLUSIONS

We have investigated the emission of neutral and ionic species from ion bombarded $\text{NaCl}\{100\}$. The mass spectra of neutral species as well as positive and negative ions have been measured. The results indicate that the mechanisms proposed for the ejection of secondary ions from electron-irradiated alkali halides are not present in the ion-bombardment process. We suggest that ions are created by direct ejection from the collision cascade.

The emission of Na_2 from $\text{NaCl}\{100\}$ has also been investigated. The data indicate that Na_2 dimers are created above the surface, in contrast to the halogen dimer emission observed in the case of electron bombardment.

The influence of the target temperature and the crystallographic structure on the TOF distributions of ejected Na atoms has been investigated. The measured spectra indicate that both collisional and electronic processes are involved in the emission of Na atoms. However, the contribution from the collision cascade is found to be higher than reported previously. Furthermore, at low temperatures, a significant delay in the thermal atom emission is observed and is attribut-

ed to the diffusion of created defects.

The discrepancy between the results obtained on polycrystalline and single-crystal samples is shown to be caused by the channeling of the incident ion and the state of the investigated surface. Our detailed investigation demonstrates clearly the importance of low dose measurements, especially on multicomponent materials.

ACKNOWLEDGMENTS

We wish to thank Professor M. Szymonski of Jagellonian University for valuable discussions. We gratefully acknowledge the financial support of the National Science Foundation and the U.S. Office of Naval Research. ZP thanks the Polish Ministry of National Education Grant No. P/04/238 for additional support.

- ¹ *Desorption Induced by Electronic Transitions, DIET 1*, edited by N. H. Tolk, M. M. Traum, J. C. Tully, and T. E. Madey (Springer, Berlin, 1983); *Desorption Induced by Electronic Transitions, DIET 2*, edited by W. Brenig and D. Menzel (Springer, Berlin, 1984).
- ² D. Pooley, Proc. Phys. Soc. **87**, 245 (1966).
- ³ N. Itoh, Nucl. Instrum. Methods B **27**, 155 (1987).
- ⁴ N. Itoh and K. Tanimura, Radiat. Effects **98**, 269 (1986).
- ⁵ R. T. Williams, Radiat. Effects and Defects in Solids **109**, 175 (1989).
- ⁶ M. Szymonski, Radiat. Effects **52**, 9 (1980).
- ⁷ T. A. Green, G. M. Loubrier, P. M. Richards, N. H. Tolk, and R. F. Haglund, Jr., Phys. Rev. B **35**, 781 (1987).
- ⁸ R. E. Walkup, Ph. Avouris, and A. P. Ghosh, Phys. Rev. B **36**, 4577 (1987).
- ⁹ T. R. Pian, M. M. Traum, J. S. Kraus, N. H. Tolk, N. G. Stoffel, and G. Margaritondo, Surf. Sci. **128**, 13 (1983).
- ¹⁰ A. Friedberg and Y. Shapira, J. Phys. C **15**, 4763 (1982).
- ¹¹ L. A. Larson, T. Oda, P. Braunlich, and J. T. Dickinson, Solid State Commun. **32**, 347 (1979).
- ¹² N. H. Tolk, M. M. Traum, J. S. Kraus, T. R. Pian, W. E. Collins, N. G. Stoffel, and G. Margaritondo, Phys. Rev. Lett. **49**, 812 (1982).
- ¹³ W. Husinsky, P. Wurz, K. Mader, E. Wolfrum, B. Strehl, G. Betz, R. F. Haglund, Jr., A. V. Barnes, and N. H. Tolk, Nucl. Instrum. Methods B **33**, 824 (1988).
- ¹⁴ M. L. Yu, D. Grischkowsky, and A. C. Balant, Appl. Phys. Lett. **39**, 703 (1981).
- ¹⁵ M. Szymonski, P. Czuba, T. Dohnalik, L. Jozofowski, A. Karawajczyk, J. Kolodziej, R. Lesniak, and Z. Postawa, Nucl. Instrum. Methods B **48**, 534 (1990).
- ¹⁶ M. Szymonski, H. Overeijnder, and A. E. De Vries, Radiat. Effects **36**, 189 (1978).
- ¹⁷ H. Overeijnder, M. Szymonski, A. Haring, and A. E. De Vries, Radiat. Effects **36**, 63 (1978); **38**, 21 (1978).
- ¹⁸ W. Husinsky, R. Bruckmuller, P. Blum, F. Viehbock, D. Hammer, and E. Barnes, J. Appl. Phys. **48**, 4734 (1977).
- ¹⁹ W. Husinsky and R. Bruckmuller, Surf. Sci. **80**, 637 (1979).
- ²⁰ *Sputtering by Particle Bombardment*, edited by R. Behrish (Springer, Berlin, 1981).
- ²¹ W. Husinsky, R. Bruckmuller, and P. Blum, Nucl. Instrum. Methods **170**, 287 (1980).
- ²² S. Miyagawa, J. Appl. Phys. **44**, 5617 (1973).
- ²³ Z. Postawa, P. Czuba, A. Poradzisz, and M. Szymonski, Radiat. Effects and Defects in Solids **109**, 189 (1989).
- ²⁴ L. S. Cota Araiza and B. D. Powell, Surf. Sci. **51**, 504 (1975).
- ²⁵ P. H. Kobrin, G. A. Schick, J. P. Baxter, and N. Winograd, Rev. Sci. Instrum. **57**, 1354 (1986).
- ²⁶ F. M. Kimock, J. D. Baxter, D. L. Papas, P. H. Kobrin and N. Winograd, Anal. Chem. **56**, 2782 (1984).
- ²⁷ C. E. Moore, *Atomic Energy Levels* (U. S. Government Printing Office National Bureau of Standards, Washington, D. C., 1971), Vol. 3.
- ²⁸ K. P. Huber, and G. Herzberg, *Constants of Diatomic Molecules* (Van Nostrand-Reinhold, New York, 1979).
- ²⁹ J. W. Rabalais, Isr. J. Chem. **22**, 365 (1982).

- ³⁰G. P. Malafsky, Ph. D. thesis, Pennsylvania State University, 1989.
- ³¹R. E. Walkup, Ph. Avouris, and A. P. Ghosh, *Phys. Rev. Lett.* **57**, 2227 (1986).
- ³²H. Overijnder, R. R. Tol, and A. E. De Vries, *Surf. Sci.* **90**, 265 (1979).
- ³³G. Betz, J. Sountheim, P. Wurz, and W. Husinsky, *Nucl. Instrum. Methods B* **48**, 593 (1990).
- ³⁴Contrary to Ref. 31, no further conclusions are drawn from the fact that the two components are needed to fit our data. A more appropriate treatment of this process is proposed in Ref. 7. The implication of this analysis to our data will be presented elsewhere.
- ³⁵M. Szymonski, J. Rutkowski, A. Poradzisz, Z. Postawa, and B. Jørgensen, in *Springer Series in Surface Science* (Springer, Berlin, 1984), Vol. 4 p. 160.
- ³⁶It has been reported (T. Madey, private communication) that H₂O does not adsorb on NaCl{100} at room temperature. To obtain any adsorption, the surface must be cooled to ~ -100 °C. This indicates that the alkali halide surfaces are relatively inert.
- ³⁷A. E. De Vries, *Nucl. Instrum. Methods B* **27**, 173 (1987).
- ³⁸N. Winograd, D. E. Harrison, and B. J. Garrison, *Surf. Sci.* **78**, 467 (1978).